Int. J. Electrochem. Sci., 1(**2006**)317-323

International Journal of ELECTROCHEMICAL SCIENCE
www.electrochemsci.org

Synthesis and Electrochemical Performance of PEO Doped Molybdenum Trioxide Nanobelts

Yanyuan Qi, Wen Chen[*]*, Liqiang Mai, Quanyao Zhu and Aiping Jin*

Institute of Materials Science and Engineering, Wuhan University of Technology, Wuhan 430070, P. R. China
[*]E-mail: chenw@mail.whut.edu.cn

Received: 31 August 2006 / *Accepted:* 7 September 2006 / *Published:* 1 October 2006

PEO doped MoO_3 nanobelts were synthesized by using a versatile hydrothermal method. The structure and morphology of the products were characterized by XRD, IR and SEM. The results indicate that PEO doped MoO_3 nanobelts with length of 1~8 μm and thickness of 50 nm can be fabricated without using any template. Compared to the pure MoO_3 nanobelts, PEO doped MoO_3 nanobelts exhibit lower discharge capacity, however, the intercalation of PEO into MoO_3 nanobelts significantly enhances the cycling stability and reversibility of insertion/extraction of Li^+ ions in the materials.

Keywords: Molybdenum trioxide, PEO, Doped, Synthesis, Electrochemical performance

1. INTRODUCTION

In recent years, there is a continuous research interest on semiconducting one-dimensional (1-D) nanomaterials because of their potential application in nanoelectronics and optoelectronics [1-3]. Great efforts have been made to develop new intercalation host-guest nanocomposite with optimal properties as materials for lithium ion secondary batteries.

MoO_3 have attracted considerable attention due to their typical two-dimensional layered structure consisting of double layers of edge- and vertex-sharing MoO_6 octahedra being weakly held together by Van Der Waals bonds. These layers can be propped open by intercalated polymers, such as Poly (p-phenylene vinylene) (PPV) [4], Poly (ethylene oxide) (PEO) [5], Polyaniline (PAN) [6], Nylon [7], etc, which enables the generation of desirable characteristics. Meantime, Poly (ethylene oxide), PEO, [(-CH_2-CH_2-O-)$_n$], has been widely used as guest materials because PEO is an ionically conductive polymer and a good solvent of alkali-metal salts and have promising cathode performance in lithium ion secondary batteries. Although many work is focused on the intercalation of PEO into MoO_3

xerogel, no attempt has been made so far to prepare PEO doped one-dimensional nanomaterials and study their electrochemical behavior.

In this paper, PEO doped MoO_3 nanobelts with length of 1~8 μm and thickness of 50 nm were synthesized by using a simple hydrothermal method. The electrochemical lithium insertion/extraction characteristic of the as-prepared nanobelts was investigated by cyclic voltammetry and a galvanostatic charge-discharge method. The results show that, when MoO_3 was modified by the intercalation of PEO, their electrochemical performance has been improved.

2. EXPERIMENTAL PART

PEO doped MoO_3 nanobelts were synthesized by the simple hydrothermal method without using any surfactant. Firstly, MoO_3 sols were prepared by the ion exchange of $(NH_4)_6Mo_7O_{24} \cdot 4H_2O$ (≥99.0 %) through a proton exchange resin and the clear light-blue MoO_3 sols (the final pH is about 2.0) were obtained. Then, the PEO was mixed with MoO_3 sols in the proportion of $(PEO)_xMoO_3$ (x=0, 0.1) to form the mixed sols. Finally, the mixed sols were directly added into a Teflon-lined autoclave and kept at 180 ^oC for 48 h. After the hydrothermal reaction, the samples were washed with distilled water and ethanol and dried at 50 ^oC for 12 h. It is worthy to note that the color of pure MoO_3 nanomaterials is light blue and that of PEO doped MoO_3 nanomaterials becomes dark blue because Mo^{6+} ions are partially reduced to Mo^{5+} to form the composition of $(PEO)_{0.1}MoO_{3-\delta}$.

The X-ray powder diffraction (XRD) measurement was performed on a D/MAX-III X-ray diffractrometer with CuK α radiation and graphite monochromator. Fourier-transformed infrared (FTIR) absorption spectra were recorded using the 60-SXB IR spectrometer with a resolution of $4cm^{-1}$. The microstructure was investigated by a JEOL-2010 scanning electron microscope (SEM) operated at 200 kV. The electrochemical properties were studied with a multichannel galvanostat/potentiostat system (MacPile). Electrochemical cells were prepared using a lithium pellet as negative electrode, 1 M solution of $LiPF_6$ in ethylene carbon (EC)/dimethyl carbonate (DMC) as electrolyte and a pellet made of the nanobelts, acetylene black and PTFE in a 10:7:1 ratio as the positive electrode. The cyclic voltammograms (CV) were measured at the scan rate of 0.5 mV/s with an Autolab model PGSTAT30 (GPES/FRA) potentiostat/galvanostat interfaced to a computer.

3. RESULTS AND DISCUSSION

3.1 XRD studies

Figure 1 shows the X-ray diffraction analysis of the products. From XRD patterns, the phase composition of the two samples are identified as pure MoO_3 (space group Pmmn; an orthorhombic cell; lattice constants a=0.396 nm, b=1.385 nm, c=0.369 nm). For the PEO doped MoO_3 nanobelts, the (020) peak shifts to the low angle, corresponding to the increase of the interlayer distance (from 0.34 nm to 0.35 nm). And the strong intensity of reflection peaks of (020), (040) and (060) indicate the anisotropic growth of both materials.

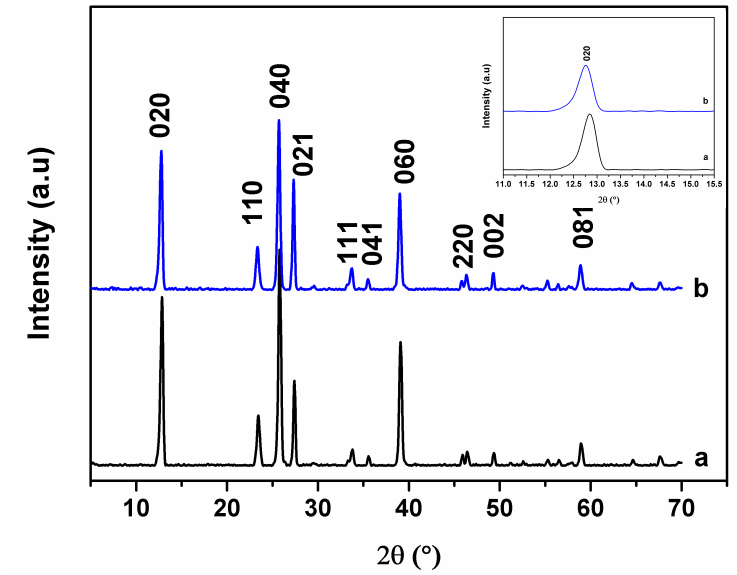

Figure 1. XRD patterns of MoO_3 (a) and $(PEO)_{0.1}MoO_{3-\delta}$ nanobelts (b). The inset is the (020) diffraction peak

3.2 IR studies

The two samples are also characterized by IR spectra as shown in Figure 2. The stretching mode of Mo-terminal oxygen is located at 999 cm^{-1}. The absorption bands at 867 cm^{-1} and 555 cm^{-1} are assigned to stretching vibrations of the $O_{(3)}$ and $O_{(2)}$ atoms linked to two and three molybdenum atoms,

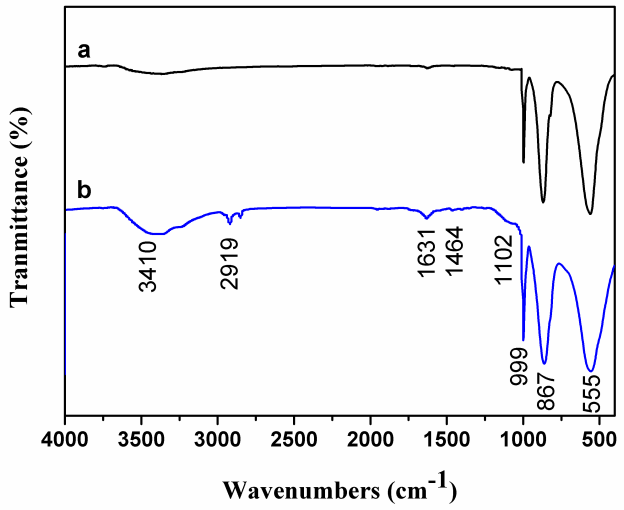

Figure 2. IR spectra of MoO_3 (a) and $(PEO)_{0.1}MoO_{3-\delta}$ nanobelts (b)

respectively [8-10]. And in the Figure 2b, the signals between 1600 and 3600 cm^{-1} in the sample are attributed to the presence of PEO. It is confirmed that PEO are successfully doped between the

interlayer of MoO_3, which results in the increase of interlayer distance. And the present of PEO have no large influence on the crystal structure of MoO_3.

3.3 SEM studies

The size and morphology of the resulting products were examined by scanning electron microscopy (SEM). As shown in Figure 3a, the pure MoO_3 nanomaterials displays a long, belt-like

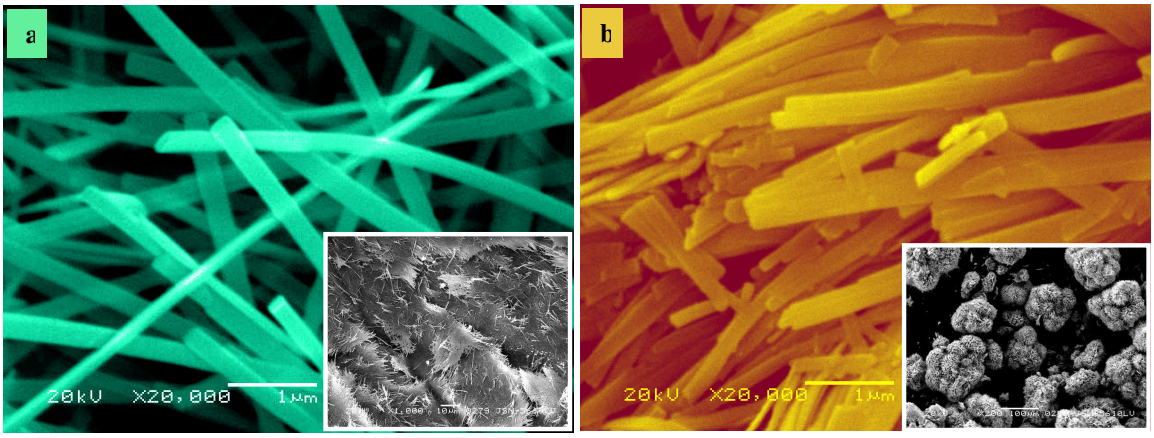

Figure 3. SEM images of PEO doped MoO_3 nanobelts. (a) MoO_3 and (b) $(PEO)_{0.1}MoO_{3-}\delta$

structure with width around 80~400 nm and length of 5~10 μm. The rectangle-like cross section of the materials is clearly visible. The average thickness of the belts is about 50 nm. For the PEO doped MoO_3 materials, it is interestingly found that the nanobelts are frequently grown together in the form of flowers (inset of Figure 3b) and the nanbelts become shorter (1~8 μm) with the presence of PEO, and the width and thickness are invariable (Figure 3b).

3.4 Electrochemical investigation

Figure 4a and 4b show cyclic voltammograms of the MoO_3 nanobelts and $(PEO)_{0.1}MoO_{3-}\delta$ nanobelts, respectively, in which the first, third and tenth cycle curves are plotted. The area A_i (i is the cycle times) which is surrounded by each cycle curve represents the amount of the Li^+ ions insertion. The cycle efficiency is calculated by the following equation:

$$Q_i = A_i / A_1$$

Where Q_i = cycle efficiency
A_1 = the area of the first cycle curve
A_i = the area of the i cycle curve

The cycle efficiency of different cycle times and materials is listed in Table 1. The third cycle efficiency Q_3 of the pure MoO_3 nanobelts and $(PEO)_{0.1}MoO_{3-\delta}$ nanobelts are 94.08 % and 95.28 %, respectively. Meantime, the tenth cycle efficiency Q_{10} of the $(PEO)_{0.1}MoO_{3-}\delta$ nanobelts is 85.69 %,

which is higher than that of MoO_3 nanobelts (69.47 %).The higher cycle efficiency of $(PEO)_{0.1}MoO_{3-\delta}$ nanobelts indicates that the stability of cycling property increases when PEO is doped into the MoO_3 nanobelts. In addition, there are two sets of (cathodic, anodic) current peaks, appearing at around the potentias (V) of (2.1, 2.65) and (2.6, 3.0) in the first cycle curve of the pure MoO_3 nanobelts (Figure 4a) and the two sets of peaks can be assigned to the insertion/extraction of Li^+ ions between the MoO_6 octahedron interlayers and intralayers [11]. And the first set of peaks (2.1, 2.65) are still observed and the peaks (2.6, 3.0) disappear in the third cycle, indicating that irreversible capacity loss due to Li^+ ions

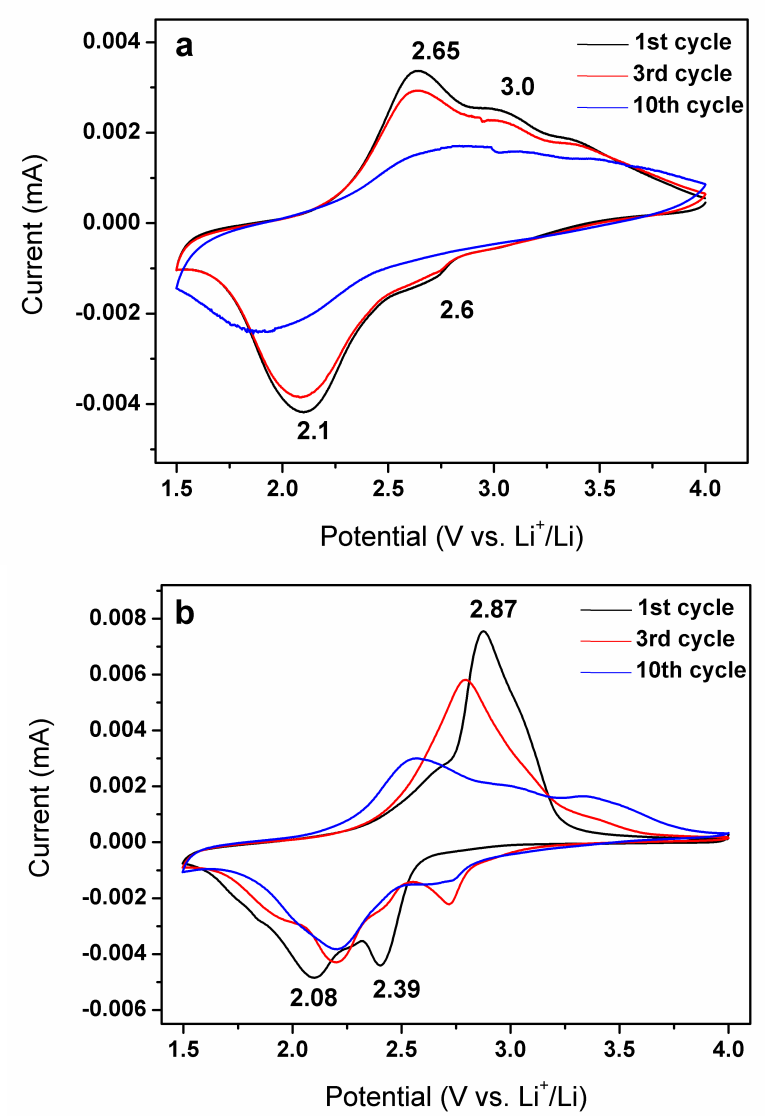

Figure 4. Cyclic voltammograms of MoO_3 nanobelts (a) and $(PEO)_{0.1}MoO_{3-\delta}$ nanobelts (b) in the first, third and tenth cycles

accommodated in MoO_6 intralayers. As to the $(PEO)_{0.1}MoO_{3-\delta}$ nanobelts, two strong peaks at 2.08 V and 2.39 V in the cathodic polarization process of the first cycle are observed (Figure 4b), corresponding to the two different intercalation process of Li^+ ions. And these two peaks are also

attributed to the insertion of lithium ions into the MoO_6 octahedron interlayer and intralayers, respectively. However, there is only one obvious peak at 2.87 V in the following anodic polarization which indicates that the lithium ions are simultaneously extracted from the MoO_6 octahedron interlayers and intralayers [12]. It is found that in the third and tenth cycles the two cathodic peaks and anodic peak still exist, indicating that the reversibility of insertion/extraction of Li^+ ions in the PEO doped MoO_3 nanoblets has been improved. More electrochemical investigations were performed to study the effect of PEO doping on electrochemical performance of MoO_3 nanobelts.

Table 1. The cycle efficiency of different cycle times and materials

Materials	Q_3	Q_{10}
MoO_3 nanobelts	94.08 %	69.47 %
$(PEO)_{0.1}MoO_{3-\delta}$ nanobelts	95.28 %	85.69 %

Figure 5 shows the curves of discharge capacity vs the cycle number for the electrodes made from MoO_3 nanobelts and PEO doped MoO_3 nanobelts at a charge-discharge current density of 30 mA/g and a temperature of 25 °C. It is apparent that the discharge capacity of pure MoO_3 nanobelts decreases

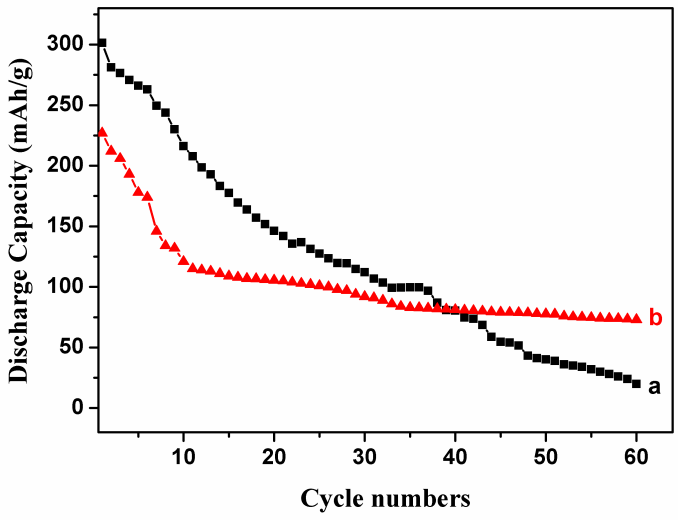

Figure 5. Cycling property of MoO_3 (a) and $(PEO)_{0.1}MoO_{3-\delta}$ nanobelts (b)

greatly with cycling, fading from 301 mAh/g in the first cycle to 26 mAh/g in the sixtieth cycle, corresponding to a capacity retention of 8.6 %. The discharge capacity of PEO doped MoO_3 nanobelts is 227 mAh/g in the first cycle, which is lower than that of pure MoO_3, but it decreases gradually in the

next cycles and the PEO doped materials still retains 73 mAh/g after sixtieth cycle, corresponding to about 32 % of its first capacity. The results are in good agreement with that obtained by CV. The discharge capacity of the PEO doped MoO_3 nanobelts becomes lower, compared with that of pure MoO_3 nanobelts, because PEO occupies some space between the interlayers which resultantly leads to a decrease of inserted Li^+ ion amount. In addition, the intercalation of PEO into MoO_3 nanobelts significantly enhances the cycling stability and reversibility of insertion/extraction of Li^+ ions because PEO has relatively strong interaction with MoO_3 interlayers and the complexing interaction with Li^+ ions, effectively shielding the electrostatic interaction between Li^+ ions and MoO_3 [13]. All these results indicate that PEO doped MoO_3 nanobelts are promising cathode materials in lithium ion batteries.

4. CONCLUSIONS

A simple and surfactant-free method is presented for the preparation of PEO doped MoO_3 nanobelts. The presence of PEO appears to decrease the length of the nanobelts, but have no large influence on the MoO_3 crystal structure. The typical width-to-thickness ratios are about 2~10. The electrochemical tests indicate that the PEO doped MoO_3 nanobelts has an initial specific capacity of 227 mAh/g, and its stabilized capacity still remained as high as 73 mAh/g after 60 cycles. The improved electrochemical performance may arise from the intercalation of PEO between the interlayers which shields the electrostatic interaction between Li^+ ions and MoO_3.

ACKNOWLEDGEMENTS

This work was supported by the National Natural Science Foundation of China (Grant No. 50372046, 50372048) and the Key Project of Chinese Ministry of Education (Grant No. 104207).

References

1. D.H.X.C. Jiang, T. Herricks and Y.N. Xia, *Nano Lett.*, 2 (2002) 1333
2. M.H. Huang, S. Mao, H. Feick, H.Q. Yan, Y.Y. Wu, H. Kind, E. Weber, R. Russo and P.D. Yang, *Science*, 292 (2001) 1897
3. P. Ball and G. Li, *Nature*, 355 (1992) 761
4. L.F. Nazar, Z. Zhang and D. Zinkweg, *J. Am. Chem. Soc*., 114 (1992) 6239
5. T.A. Kerr, H. Wu and L.F. Nazar, *Chem. Mater*., 8 (1996) 2005
6. E. Ruiz-hitzky, P. Aranda and B. Casal, *J. Mater. Chem*., 2 (1992) 581
7. Y.J. Liu, D.C. Decroot and J.L. Schindler, *Adv. Mater*., 5 (1995) 369
8. G. Guzman, B. Yebka, J. livage and C. Julien, *Solid State Ionics,* 407 (1996) 86
9. W. Dong and B. Dunn, *J. Non-Cryst Solids*, 225 (1998) 13
10. G. A. Nazri and C. Julien, *Solid State Ionics*, 80 (1995) 271
11. T. Tsumur and M. Inagaki, *Solid State Ionics*, 104 (1997) 183
12. Y. Iriyanma, T. Abe, M. Inaba and Z. Ogumi, *Solid State Ionics,* 10 (2000) 95
13. L. F. Nazar, H. Wu and W.P. Power, *J. Mater. Chem.*, 5 (1995) 1985